

Hybrid structural arrangements mediate stability and feasibility in mutualistic networks

Aniello Lampo

Universitat Rovira i Virgili, Tarragona, Catalonia, Spain

María J. Palazzi and Javier Borge-Holthoefer

Internet Interdisciplinary Institute (IN3), Universitat Oberta de Catalunya, Barcelona, Catalonia, Spain

Albert Solé-Ribalta

*Internet Interdisciplinary Institute (IN3), Universitat Oberta de Catalunya, Barcelona, Catalonia, Spain and
URPP Social Networks, University of Zurich, Zurich, Switzerland*

(Dated: July 7, 2021)

Perhaps the largest debate in network Ecology, the emergence of structural patterns stands out as a multifaceted problem. To the methodological challenges –pattern identification, statistical significance– one has to add the relationship between candidate architectures and dynamical performance. In the case of mutualistic communities, the debate revolves mostly around two structural arrangements (nestedness and modularity) and two requirements for persistence, namely feasibility and stability. So far, it is clear that the former is strongly related to nestedness, while the latter is enhanced in modular systems. Adding to this, it has recently become clear that nestedness and modularity are antagonistic patterns –or, at the very least, their coexistence in a single system is problematic. In this context, this work addresses the role of the interaction architecture in the emergence and maintenance of both properties, introducing the idea of hybrid architectural configurations. Specifically, we examine in-block nestedness, compound by disjoint subsets of species (modules) with internal nested organization, and prove that it grants a balanced trade-off between stability and feasibility. Remarkably, we analyze a large amount of empirical communities and find that a relevant fraction of them exhibits a marked in-block nested structure. We elaborate on the implications of these results, arguing that they provide new insights about the key properties ruling community assembly.

I. INTRODUCTION

After decades applying random matrix theory to the study of ecological communities, the evidence that interactions among species are not randomly assembled, but manifest instead clear architectural patterns, subverted the field from then onwards. While network theory has developed efficient methods to detect those patterns in faster and more reliable ways, ecologists strived to decipher the relationship between the observed structural arrangements and several dynamical properties of ecosystems [1–11].

In this way, for example, the identification of nested arrangements in real mutualistic networks [12, 13] prompted a myriad of works linking the emergence of such pattern to certain beneficial properties, *e.g.*, the promotion of diversity [14], the maximization of species abundances [5] or the feasibility of such ecosystem [7, 8], the range of conditions leading to positive abundances for all biotas. This beautifully simple path –the idea that a single pattern could mediate many desirable features– was, however, debased by the evidence that nested networks are less likely to be stable [3, 6]; and further challenged as the stabilizing effects associated to modularity [4, 9, 10] were ascertained. To reconcile both perspectives, one could consider the possibility that a mutualistic network (*e.g.*, plant-pollinator) exhibits both a nested and a modular structure, as suggested in [15]. Unfortu-

nately, empirical [16] and later analytical [17] evidence showed that these two patterns may not be structurally compatible with each other, pushing this path to a dead-end.

Thus, so far, the study of the structure-dynamics interplay has mostly been centered –with exceptions [18, 19]– on one-to-one mappings. That is, examining the correspondence of a given dynamical property to a single architectural pattern, or viceversa. However, this view may be too limited to fit some of the complex dynamics of natural systems, which seem to evolve concurrently optimizing several ecological variables [20, 21]. A multi-objective analysis of ecological systems is largely unexplored.

Here, we take this research direction to analyze how hybrid structural arrangements may suffice to accommodate dynamical properties typically ascribed to incompatible structural signatures. Hybrid, compound, or in-block nested (IBN) structures (compartmentalized networks whose modules are internally arranged following a nested pattern) were first hypothesized over a decade ago [22] and thereon found in empirical settings [23–25], also outside ecology [26]. Together with the advances in network-theoretical aspects [17, 27, 28], there are some clues on the dynamics leading to the emergence of IBN [29, 30], including generalized Lotka-Volterra systems [31, 32]. Using this latter framework, in this article, we focus primarily on the performance of a large

ensemble of synthetic networks with regards to stability and feasibility, showing that IBN structures exhibit a balanced trade-off between both features, so necessary to ensure community persistence, meant as the system capability to stably sustain a large number of species. Then, we analyze approximately one hundred mutualistic empirical networks, and find that a large fraction of them exhibits a significant degree of IBN – often higher than any other structural arrangements. These results suggest that, in many systems, the emergence of hybrid interaction patterns responds to the attempt to preserve both stability and diversity, rather than promoting one over the other.

II. METHODS

To validate our hypothesis, we need to compare the performance of different structural arrangements (namely modular, nested and in-block nested, see Fig. 1) with regards to stability and feasibility, modelling their evolution with the standard Lotka-Volterra equations, which can jointly encode specific mutualistic and competitive relations among species. In this section, we first outline the specificities of the dynamical framework, which govern the evolution of the system; we then proceed to detail the procedure to generate an ensemble of synthetic networks with controlled architecture; and finally the methods to evaluate stability and feasibility are presented.

A. Generalized Lotka-Volterra dynamics

The interaction of species in ecosystems is usually modeled as a network in which nodes represent species, and edges encode the interaction type and strength among them: a link in the adjacency matrix representing the network, M_{ij} , is turned on if species i and j interact. Positive values of adjacent matrix typically indicate mutualistic relations, and negative values competitive ones. On the basis of this interaction network, species abundances can be mapped to a set of time-dependent functions $x_i(t)$, and their temporal evolution is commonly studied by recalling the generalized Lotka-Volterra equation

$$\frac{dx_i}{dt} = x_i \left(r_i - \sum_j M_{ij} x_j \right), \quad (1)$$

where the indexes i and j run over the system species. The parameters r_i represent the intrinsic growth rate coefficients, ruling the dynamics of the i -species when interspecific interaction is dropped out.

In bipartite mutualistic networks, we further differentiate species in two groups, A and P . Relations between species of different groups are assumed to be mutualistic, and competitive within group. Many ecosys-

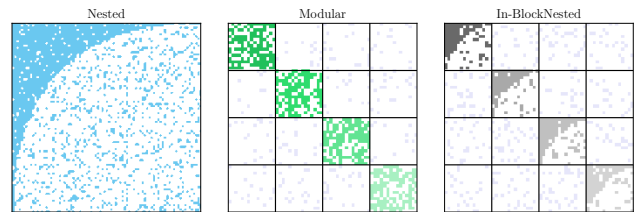


FIG. 1. Examples of adjacency matrices of networks associated to nested (left) modular (middle) and IBN (right) structures. In each of the three matrices shown, each row represents species of group A and each column represents a species of group P , while entries portray the mutualistic interaction links between the two groups. In the nested networks, the more specialist species interact only with sets of those interacting with the more generalists, and the related adjacency matrices manifest the traditional triangular structure. Modular networks are compound by weakly interlinked groups of species (modules) with strongly internal connectivity, and this yield an adjacency matrix divided in blocks. IBN matrices are divided in blocks with an internal nested structure.

tems can be represented by these type of networks, e.g. plant-pollinators or seed-dispersal, in which species belonging to different guilds cooperate, but compete for resources with those in the same guild. Noteworthy, many datasets are available to study real mutualistic communities [33]. For the sake of simplicity, during the rest of the manuscript we will assume that both sets of species, A and P , have the same cardinality $|A| = |P| = S$. For these bipartite ecosystems, the adjacency matrix describing species relation exhibits a particular shape,

$$M = \begin{pmatrix} \Omega_{AA} & -\Gamma_{AP} \\ -\Gamma_{PA} & \Omega_{PP} \end{pmatrix}. \quad (2)$$

Block Ω^{AA} (Ω^{PP}) represents the competitive interactions between species corresponding to the set A (P), and the block Γ^{AP} describes the mutualistic interaction between species corresponding to different sets. Both interaction matrices, Ω and Γ may have a particular structure or else be unstructured (random).

B. Synthetic network generation

The main objective of our paper is to study the dynamical properties of hybrid mutualistic interactions, such as in-block nested arrangements, in comparison to the performance offered by classical arrangements such as nested and modular structures. Thus, off-diagonal blocks of matrix M , Γ^{AP} and Γ^{PA} , can take three different structural arrangements: modular, nested and in-block nested. On the contrary, following the state-of-the-art [3, 5, 8], the diagonal blocks of matrix M are treated as unstructured and assumed to be fully connected.

To construct a rich synthetic ensemble controlling for the different structural patterns of Γ^{AP} at stake, it is

convenient to use the model in [26, 27], which spans nested, modular and IBN configurations. The model depends on four tunable parameters: the number of modules $B \in [1, \infty)$, the inter-module noise $\mu \in [0, 1]$, the amount of nested order within modules $p \in [0, 1]$, and a shape parameter controlling the slimness of the nested structure $\xi \in [1, \infty]$. From the model's perspective, the nested matrix in Fig. 1 (left) corresponds to $B = 1$, $p = 0.25$ and $\xi = 1$; the modular and IBN matrices (center and right) correspond to $B = 4$, $\mu = 0.25$ and $\xi = 1$, the difference being that $p = 1$ in the modular panel, while $p = 0.25$ in the IBN one. Through the article the different degree of nestedness, modular structure and in-block nestedness will be quantified using the variation of the NODF measure as defined in [27], the modularity optimized by means of the extremal optimization algorithm [34] and in-block nestedness optimized as defined in [27]. See Sec. S1 of the Supporting Information for details.

For varying size $S \in [20, 120]$ and connectance $C \in [0.04, 0.3]$ values, we build three sets of 54 matrices each, corresponding to the architectures of interest. As we will describe below, parameter ranges for S and C are chosen to be compatible with real empirical mutualistic networks (see Fig. S4 of the Supporting Information). In some cases, we randomly removed or added links to the networks until the desired connectance values were met. This large ensemble –around 38×10^3 networks for each pattern– allows for a fine-grained analysis of the relationship between the three structural patterns, at fixed size and connectance, and several dynamical properties of the ecosystem.

Besides their internal structure, the weights of both, the competitive and mutualistic interaction, are assumed to be centered around a mean value:

$$\Gamma_{ij}^{AP} = g_{ij}a_{ij}, \quad g_{ij} = \gamma + \sigma_{ij}^\gamma, \quad \sigma_{ij}^\gamma \ll \gamma. \quad (3)$$

Here, $a_{ij} = 1$ if there exists a link between species i and j , zero otherwise. The quantity g_{ij} is the interaction strength and is expressed as the result of a small perturbation σ_{ij}^γ around a mean value $\gamma = \langle \gamma_{ij} \rangle$. Matrices Γ^{PA} , Ω^{AA} and Ω^{PP} are treated similarly, except for the competition between the same species which is set to one ($M_{ii} = 1$).

Statistics regarding the spanned nestedness, modularity and IBN values by the generated dataset are provided in Fig. S1 of the Supporting Information.

C. Stability

During the last decades there has been a profusion of metrics aimed to assess stability [35]. Here, we focus on the concept of local asymptotic stability (hereafter stability), defined as the system capability to restore the original equilibrium state after infinitesimal perturbation of abundancies. This may be evaluated by looking into the

Jacobian matrix of the generalized Lotka-Volterra model,

$$J_{ij} \equiv \left(\frac{\partial \dot{x}_i}{\partial x_j} \right)_{\mathbf{x}=\mathbf{x}^*}, \quad (4)$$

where \mathbf{x}^* represents the stationary state of Eq. (1), defined by the condition $\dot{x}_i^* = 0$ and leading to

$$\mathbf{x}^* = M^{-1}\mathbf{r}, \quad (5)$$

which describes the species abundances at equilibrium. Replacing Eq. (1) into Eq. (4) and recalling Eq. (5) we reach the final form of the Jacobian matrix of the Lotka-Volterra model:

$$J_{ij} = -x_i^* M_{ij}. \quad (6)$$

The system is stable if the real part of the largest eigenvalue of the Jacobian matrix is negative, otherwise is said to be unstable. Hence, the quantity

$$\lambda^* = -\text{Max}[Re\{\lambda_J\}], \quad \lambda_J \in \text{Sp}(J) \quad (7)$$

naturally describes the stability of the system and can be used to assess how different systems compare regarding stability.

As said, the Jacobian matrix provides information about the long-time response of the first-order dynamical behavior of the system, after infinitesimal perturbations of the stationary abundancies. These in general affect the expression of the Jacobian and have to be taken into account in the eigenvalues calculation, as seen in Eq. (6). Following the approach presented in [36], we assume that the abundancies are all positive, *i.e.* $x_i^* > 0 \forall i \leq 2S$ which is equivalent to sample a proper \mathbf{r} vector in the feasibility domain.

D. Feasibility

Feasibility refers to the conditions of the external parameters which yield a stationary state in which all species abundancies are positive, *i.e.* $x_i > 0, \forall i \leq 2S$. In the case of the Generalized Lotka-Volterra model, Eq. (1), it is easy to infer that, once M is fixed, feasibility depends solely on the self-growth vector \mathbf{r} . Thus, the feasibility space is spanned by the self-growth rates leading to positive abundancies, and takes the form of a cone whose borders are given by the column vectors of M [8, 37, 38].

The degree of feasibility is thus provided by the openness of this cone, *a.k.a.* the related solid angle Θ , which is completely determined by the M matrix. Beyond its geometric meaning, properly normalized, Ω may be interpreted as the probability of randomly sampling an \mathbf{r} vector conducive to positive abundancies. This quantity has been calculated in [39] and takes the following form:

$$\Theta = \frac{1}{(2\pi)^{S/2} \sqrt{\det(\Sigma)}} \int \dots \int_{\mathbb{R}^S \geq 0} e^{-\frac{1}{2}\mathbf{x}^t \Sigma^{-1} \mathbf{x}} d\mathbf{x}, \quad (8)$$

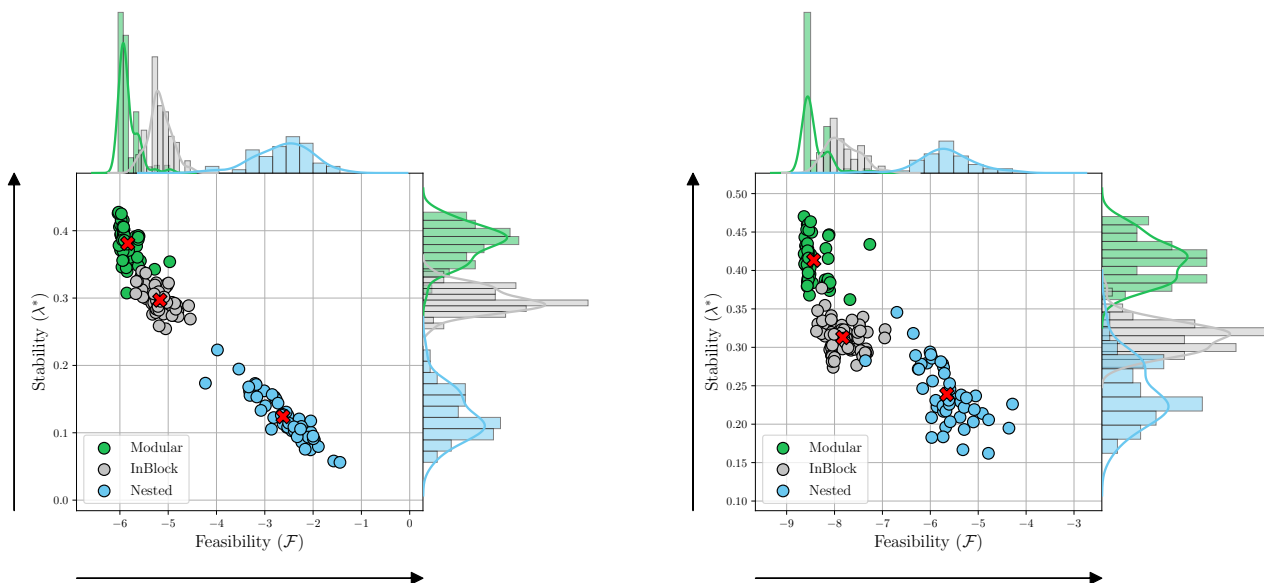


FIG. 2. Stability and Feasibility values for an ensemble of synthetic networks with in-block, nested, and modular architecture, with $S = 20$ species and connectance $C = 0.2$. The plot on the left describes a pure mutualistic context ($\gamma = 0.13$, $\omega = 0$) while that on right includes intra-guild competition with the same parameters values employed in [8], $\gamma = 0.13$, $\omega = 0.01$. Each point represents a network: its horizontal coordinate is given by the feasibility \mathcal{F} introduced in Sec. IID, while the vertical one is provided by the quantity λ^* defined in Eq. (7). It is possible to recognize three different clusters corresponding to different structures: nested and modularity respectively promote feasibility and stability, while IBN trades-off the two properties. Red daggers are located at the average values of stability and feasibility of the corresponding network clusters.

which corresponds to the cumulative function of a multivariate normal distribution with mean value equal to zero and variance matrix $\Sigma^{-1} = 2M^t M$. The solid angle of the feasibility space can be easily obtained by using the methods and code in [8]. Hereafter, as usual, we will represent the solid angle on a logarithmic scale $\mathcal{F} \equiv \log_{10}(\Theta)$. This is the final quantity we will refer under the term feasibility. It turns that $-\infty < \mathcal{F} \leq 0$ because $0 \leq \Theta \leq 1$, since it is a normalized distribution. The higher the value of \mathcal{F} , the larger the likelihood of finding a feasible system.

III. RESULTS

In this section, we first present results regarding the stability and feasibility of synthetic structured ecosystems, highlighting the balanced performance of IBN networks. We then turn our attention to real ecosystem communities, and show that a significant fraction of them actually exhibit IBN arrangements, falling within the parameter range found to balance stability and feasibility.

A. Stability and feasibility of structured synthetic networks

The results regarding the stability and feasibility for nested (\mathcal{N}), in-block nested (\mathcal{I}), and modular (\mathcal{Q}) synthetic networks are presented in Fig. 2, for several systems of size $S = 20$ and connectance $C = 0.2$. Obvious to the naked eye, ecosystems with modular structure are most stable ones, while nestedness penalizes stability. In this sense, stability defines a hierarchy in which modular networks are on the top, nested ones on the bottom and IBN structures lay between those. Similarly, on the x-axis, feasibility shows a similar behavior, at odds with stability: nested architectures show the highest values of \mathcal{F} , while modular ones fall clearly behind. Importantly, in both situations IBN offers intermediate dynamical properties, emerging as a natural trade-off between stability and feasibility. Summarizing, we have

$$\langle \mathcal{F}_{\mathcal{N}} \rangle > \langle \mathcal{F}_{\mathcal{I}} \rangle > \langle \mathcal{F}_{\mathcal{Q}} \rangle, \quad \langle \lambda_{\mathcal{N}}^* \rangle < \langle \lambda_{\mathcal{I}}^* \rangle < \langle \lambda_{\mathcal{Q}}^* \rangle, \quad (9)$$

where $\langle \mathcal{F}_{\mathcal{X}} \rangle$ indicates the average value of feasibility over an ensemble of synthetic networks with predominant \mathcal{X} structure. Similarly for $\langle \lambda_{\mathcal{X}}^* \rangle$. These values are highlighted with red crosses in Fig. 2.

Our results regarding nested and modular ecosystems agree with the previous literature, where nestedness was

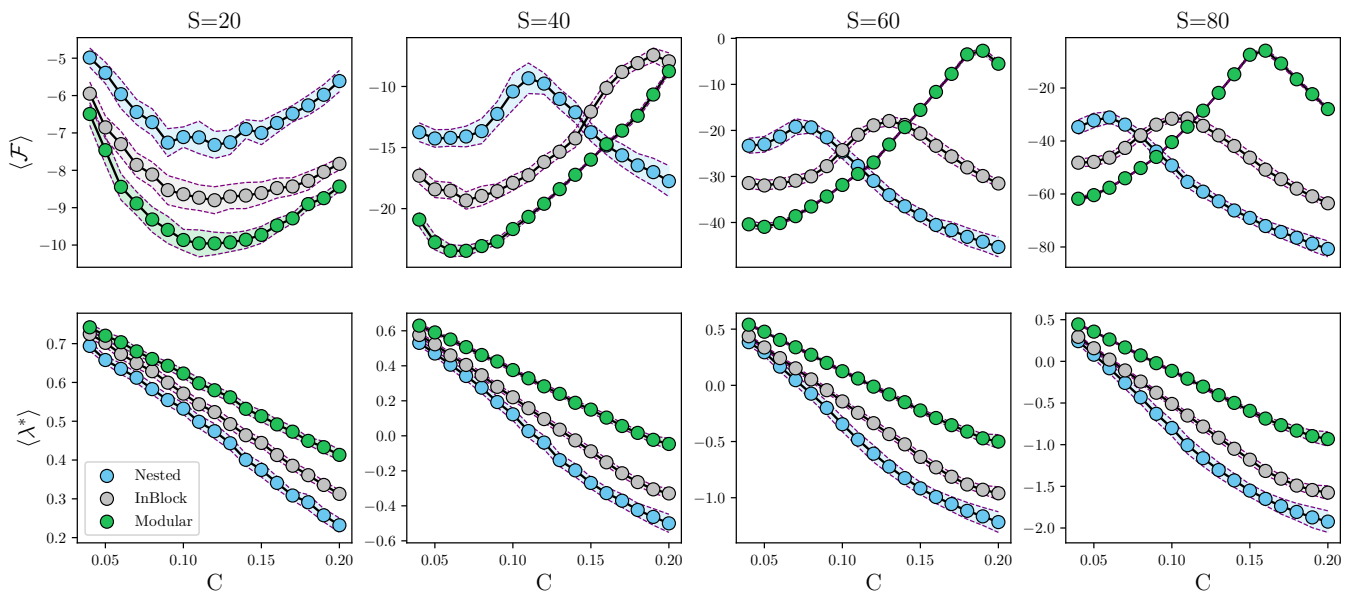


FIG. 3. Stability and Feasibility dependence on the connectance for nested, in-block and modular networks, for ecosystems of different sizes. Each point refers to a set of matrices of fixed connectance, and is located at the resulting average value of feasibility (up) or stability (down). Shadow areas provide an information about the variance. All the plots refer to the $\gamma = 0.13$ and $\omega = 0.01$.

found to hinder stability [3, 6] favoring feasibility [8]; and modularity was found to boost stability [9], while its effects on feasibility remained untested so far. From the mathematical point of view, the stability behavior we detect may be understood in terms of the Gershgorin theorem [40], linking the real part of the largest eigenvalue with the row sum of the interaction matrix, which is maximized in nested networks because of the presence of generalist species (see Sec S2 of the Supporting Information). This is certainly true for pure mutualistic systems [3] but, worth highlighting, these results seem to be robust for an average competition strength up to 10% of the mutualistic one.

The results presented so far are limited to fixed values of connectance and species number. We extend this analysis to a wider parameter range in Fig. 3. Each column of the figure corresponds to a system size S , where connectance C is confronted with average feasibility $\langle \mathcal{F} \rangle$ (top) and average stability $\langle \lambda^* \rangle$ (bottom). Overall, one can safely conclude that, almost in all parameter range, IBN structures offer a balanced performance to jointly optimize stability and feasibility, confirming in this sense the main hypothesis set on this paper. This is certainly true for stability, where IBN is always the second-best architecture (behind modularity), no matter the size or connectance of the system.

The case of feasibility, however, suggests a more complex scenario, because of the non-monotonic behavior of $\langle \mathcal{F} \rangle$ as C grows, in the case of nested and IBN structures. These phenomena may find its roots in the relative difference between effective and critical competition, as it

was shown for structural stability in [11]. Still, this non-monotonic dependence demands further analysis, and lies beyond the scope of this work.

Whichever the underlying cause of this phenomena, it is easy to see that the three structures become optimal $\langle \mathcal{F} \rangle$ -wise within some parameter range. For instance, nested structures are optimal for $C \in (0.04, 0.10]$, IBN structures for $C \in (0.10, 0.15]$ and modular structures for $C \in (0.15, 0.20]$ in Fig. 3 for $S = 60$. This suggests the existence of three regimes, in which (a) IBN offers a trade-off between feasibility and stability, (b) IBN offers advantage with respect to feasibility, and balance on stability and (c) modular networks maximize feasibility and stability. Note that in two of these regimes, IBN structural arrangements are more beneficial than any of its non-hybrid counterparts. See also results in Sec. S3 and Figs. S2 of the Supporting Information for the pure mutualistic case. Results and conclusions derived from Fig. 3 hold as well.

Overall results show that the balanced performance of IBN is not universal and concerns a finite, albeit significant, portion of the parameters space, mainly related to small values of connectance or species number. However, as we will see in the following section, this region integrates practically all real mutualistic ecosystems considered in this paper.

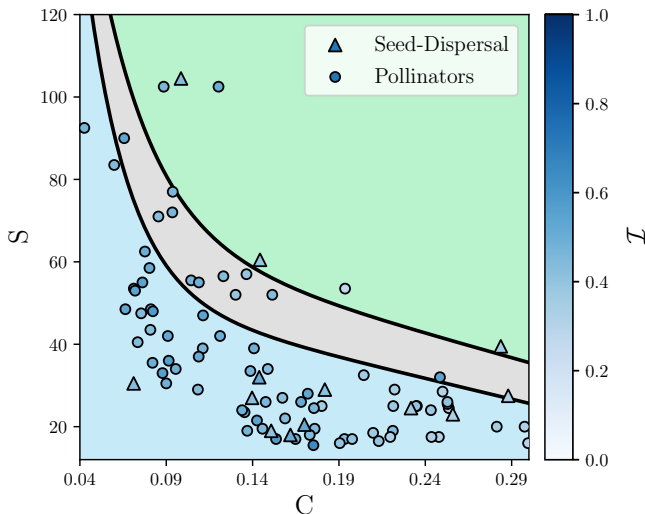


FIG. 4. Validity of the trade-off property of IBN in the size-connectance domain, with $\gamma = 0.13$ and $\omega = 0.01$. Blue, grey and green areas, experimentally obtained, refer to the region in which the nested, in-block, and modular networks maximize feasibility. Specifically, in the blue region the condition in Eq. 9 is fulfilled and IBN constitutes a trade-off between stability and feasibility. Scatter plot depicts the distribution of empirical pollinators and seed-dispersal mutualistic communities of [33], with color portraying the in-block nestedness degree.

B. In-block nestedness in empirical networks

To validate our findings on real mutualistic ecosystems, we analyze the predominant structural arrangements of the plant-pollinator and seed-dispersal communities from the *Web of Life* database [33]. These networks range over a large domain of size and connectance aligned with the synthetic analysis we provide in the previous section. Since our objective is to focus on a representative set of ecosystems with common properties, not on those with exceptional ones which should be analyzed individually, we excluded from our analysis several networks of the Web of Life. These include very small ecosystems and communities with very large or very small C and S , considering its distribution. See Sec. S4 of the Supporting Information for further details. We finally end up with a dataset of 74 real communities. Details on the selected networks can be found in Table S1 of the Supporting Information.

In the previous subsection we showed that the relationship between feasibility and network architecture is not uniform, depends on the size and connectance of the network, and describes different regimes. Fig. 4 overlays the empirical communities over the phase diagram representing these regimes. We see that more than 93% of real networks fall within regime (a) or (b), that is, the S - C region where IBN outperforms modularity and nestedness to jointly cope with stability and feasibility, thus being

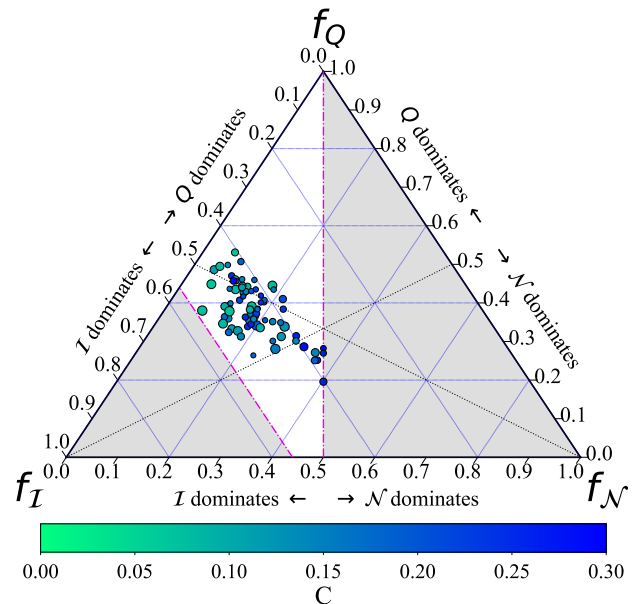


FIG. 5. Distribution of pollinator and seed-dispersal empirical networks selected from [33], across a ternary plot. The colorbar indicates the networks connectance, evaluated according the measure introduced in [27]. The point size provides information regarding the number of species of the corresponding community.

an advantageous interaction architecture to promote ecological persistence. This, however, does not imply *per se* that these real networks are arranged as IBN structures.

The next –and final– step is then to explore which type of arrangement is predominant in those empirical networks: modular, nested, or in-block nested. Results comparing the presence of the different patterns within single ecosystems are given in the ternary plot (or simplex) of Fig. 5. Each mutualistic network is represented in the plot on a three coordinate space, corresponding to the different values obtained by maximizing IBN’s fitness function (\mathcal{I}), modularity (Q), or by measuring nestedness (\mathcal{N}), as defined in Sec. S1 of the Supporting Information. See also Table S1 for values we obtained for each specific network. Specifically, on the ternary plot, each network is represented by a vector $(f_{\mathcal{N}}, f_Q, f_{\mathcal{I}})$, where as $f_{\mathcal{N}} = \mathcal{N}/(\mathcal{N}+Q+\mathcal{I})$, and similarly for $f_Q, f_{\mathcal{I}}$. For visual aid, the plot is divided into “dominance regions” (angle bisectors), i.e. areas of the simplex where either pattern is stronger than the other two. Also, note that shadowed gray areas are necessarily empty, given the structural constraints mentioned in Sec. S1 of the Supporting Information and carefully discussed in [26]. Remarkably, the ternary plot unveils that most ecological communities –especially those with low-to-mid connectance– fall into the IBN area.

Additionally, Fig. S5 of the Supporting Information statistically assess the emergence of the individual ar-

rangements with respect to a null model. In this case, we used the Curveball algorithm in [41]. Solely by looking into the statistical analysis, we can see that most of the analyzed communities display significant IBN structure, in comparison to the results obtained for nested and modular arrangements. Intriguingly, considering this null model only a few networks exhibit a significant modular structure. Worth highlighting, IBN significance is appreciable despite of the restrictive character of the Curveball algorithm.

IV. DISCUSSION

Stability and feasibility have been mapped, in the past, onto single preferential architectural patterns. However, the interest in studying abundant, diverse and stable ecological communities calls for a new vision of species interaction patterns, able to reproduce the balance of several properties, rather than the predominance of a single one. With this objective, we leave the traditional approach focused on a single architectural pattern, and look into compound structures. We consider the in-block nested configuration, where nestedness and modularity interfere at a network's mesoscale, and show that it provides an optimal trade-off between stability and feasibility. Moreover, the analysis of real mutualistic networks proves that a large fraction of them actually exhibits an in-block nested organization.

Recently, in-block nestedness has attracted notable attention as an emergent architecture, which unfolds from an abundance-maximization process [5] on top of a niche-structured population [31, 32], providing a bottom-up perspective on nestedness-modularity coexistence.

Our results have important consequences on the general understanding of the mechanisms ruling the organization of mutualistic communities. So far, the question has been addressed as finding *the key property* shaping ecosystems assemblage.

For instance, Saavedra *et al.* [8] conclude that communities promote feasibility over stability, but not both at the same time. A similar reasoning applies for the

pair stability-modularity. The introduction of an intertwined architecture permits to revisit and deepen this finding. Particularly, the emergence of in-block nestedness in real communities, associated now to a trade-off between stability and feasibility, implies that the fundamental criterium underlying the assembly process is the equilibrium between those (and possibly more) properties, rather than the predominance of one of them.

The mediating role of in-block nestedness depends in general on the connectance and species number. In small and very sparse communities, nestedness may suffice to guarantee a feasible and stable system. For large and dense communities, we detect an unexpected effect consisting in a reversing of the feasibility hierarchy. Only in this regime, both stability and feasibility result to be promoted by modularity, which stands out as the optimal pattern for ecosystems assemblage. Then again, empirical networks in the modular-optimal range are very scarce. All in all, our results indicate that there may be different structural adaptations that can serve the need of mutualistic communities to be both feasible and stable, as they evolve into larger (smaller) or denser (sparser) systems. This idea can contribute to our understanding of ecosystems assembly processes, in which an optimal size-connectance-architecture relationship may be relevant.

Along the same line, one could look into the extension of our analysis beyond Lotka-Volterra dynamics in Eq. (1), characterized by an interaction term depending linearly on the M matrix. This dynamics is largely employed in the literature, but so is its non-linear extension, the communities, associated Holling type II. The physical difference between the two frameworks lies in the interaction (or handling) time: it is neglected in the linear case, but not so in the other. Therefore, the magnitude of such a timescale introduces a bound on the validity of the theory we presented. This is certainly available when such a time tends to zero. For finite non-zero values, one may proceed perturbatively provided that those values are small. Still, it is possible to show that, as handling time tends to the infinity, the resulting equation may be cast in a linear form. Nevertheless, the effect of intermediate values of the handling time represents an open question.

-
- [1] T. Okuyama and J. N. Holland, *Ecology Letters* **11**, 208 (2008).
 - [2] E. Thébault and C. Fontaine, *Science* **329**, 853 (2010).
 - [3] S. Allesina and S. Tang, *Nature* **483**, 205 (2012).
 - [4] D. B. Stouffer and J. Bascompte, *Proceedings of the National Academy of Sciences* **108**, 3648 (2011).
 - [5] S. Suweis, F. Simini, J. R. Banavar, and A. Maritan, *Nature* **500**, 449 (2013).
 - [6] P. P. Staniczenko, J. C. Kopp, and S. Allesina, *Nature communications* **4**, 1391 (2013).
 - [7] R. P. Rohr, S. Saavedra, and J. Bascompte, *Science* **345**, 1253497 (2014).
 - [8] S. Saavedra, R. Rohr, J. Olesen, and J. Bascompte, *Ecology and evolution* **6**, 1007 (2015).
 - [9] S. Allesina, J. Grilli, G. Barabás, S. Tang, J. Aljadeff, and A. Maritan, *Nature Communications* **6**, 7842 (2015).
 - [10] J. Grilli, T. Rogers, and S. Allesina, *Nature Communications* **7**, 12031 (2016).
 - [11] A. Pascual-García and U. Bastolla, *Nature Communications* **8**, 1 (2017).
 - [12] J. Bascompte, P. Jordano, C. J. Melián, and J. M. Olesen, *Proceedings of the National Academy of Sciences*

- 100**, 9383 (2003).
- [13] M. S. Mariani, Z.-M. Ren, J. Bascompte, and C. J. Tessone, *Physics Reports* **813**, 1 (2019), nestedness in complex networks: Observation, emergence, and implications.
- [14] U. Bastolla, M. A. Fortuna, A. Pascual-García, A. Ferrera, B. Luque, and J. Bascompte, *Nature* **458**, 1018 (2009).
- [15] J. M. Olesen, J. Bascompte, Y. L. Dupont, and P. Jordano, *Proceedings of the National Academy of Sciences* **104**, 19891 (2007).
- [16] M. A. Fortuna, D. B. Stouffer, J. M. Olesen, P. Jordano, D. Mouillot, B. R. Krasnov, R. Poulin, and J. Bascompte, *Journal of animal ecology* **79**, 811 (2010).
- [17] M. Palazzi, J. Borge-Holthoeffer, C. Tessone, and A. Solé, *J.R. Soc. Interface* **16**, 20190553 (2019).
- [18] C. A. Serván, J. A. Capitán, J. Grilli, K. E. Morrison, and S. Allesina, *Nature ecology & evolution* **2**, 1237 (2018).
- [19] C. Carpentier, G. Barabás, J. W. Spaak, and F. De Laender, *Nature Ecology & Evolution*, 1 (2021).
- [20] D. Tilman and J. Downing, *Nature* **367**, 363 (1994), copyright: Copyright 2018 Elsevier B.V., All rights reserved.
- [21] K. S. McCann, *Nature* **405**, 228 (2000).
- [22] T. M. Lewinsohn, P. Inácio Prado, P. Jordano, J. Bascompte, and J. M. Olesen, *Oikos* **113**, 174 (2006).
- [23] C. O. Flores, J. R. Meyer, S. Valverde, L. Farr, and J. S. Weitz, *Proceedings of the National Academy of Sciences* **108**, E288 (2011).
- [24] C. O. Flores, S. Valverde, and J. S. Weitz, *The ISME Journal* **7**, 520 (2013).
- [25] S. J. Beckett and H. T. Williams, *Interface Focus* **3**, 20130033 (2013).
- [26] M. J. Palazzi, J. Cabot, J. L. Cánovas Izquierdo, A. Solé-Ribalta, and J. Borge-Holthoeffer, *Scientific Reports* **9**, 2045 (2019).
- [27] A. Solé-Ribalta, C. J. Tessone, M. S. Mariani, and J. Borge-Holthoeffer, *Physical Review E* **96**, 062302 (2018).
- [28] M. S. Mariani, M. J. Palazzi, A. Solé-Ribalta, J. Borge-Holthoeffer, and C. J. Tessone, *Communications in Non-linear Science and Numerical Simulation* **94**, 105545 (2021).
- [29] R. B. Pinheiro, G. M. Felix, C. F. Dormann, and M. A. Mello, *Ecology* **100**, e02796 (2019).
- [30] M. A. Mello, G. M. Felix, R. B. Pinheiro, R. L. Muylaert, C. Geiselman, S. E. Santana, M. Tschapka, N. Lotfi, F. A. Rodrigues, and R. D. Stevens, *Nature ecology & evolution* **3**, 1525 (2019).
- [31] W. Cai, J. Snyder, A. Hastings, and R. M. D'Souza, *Nature Communications* **11** (2020), <https://doi.org/10.1038/s41467-020-19154-5>.
- [32] M. J. Palazzi, A. Solé-Ribalta, V. Calleja-Solanas, S. Meloni, C. A. Plata, S. Suweis, and J. Borge-Holthoeffer, *Nature communications* **12**, 1 (2021).
- [33] "Web of life: ecological networks database," <http://www.web-of-life.es/>.
- [34] J. Duch and A. Arenas, *Physical review E* **72**, 027104 (2005).
- [35] S. Kéfi, V. Domínguez-García, I. Donohue, C. Fontaine, E. Thébault, and V. Dakos, *Ecology Letters* **22**, 1349 (2019).
- [36] T. Gibbs, J. Grilli, T. Rogers, and S. Allesina, *Phys. Rev. E* **98**, 022410 (2018).
- [37] I. Svirezhev and D. O. Logofet, *Stability of biological communities* (Mir Publisher, 1983).
- [38] J. Grilli, M. Adorisio, S. Suweis, G. Barabás, J. R. Banavar, S. Allesina, and A. Maritan, *Nature Communications* **8**, 14389 (2017).
- [39] J. M. Ribando, *Discrete and Computational Geometry* **36**, 479 (2006).
- [40] R. S. Varga, *Gerschgorin and His Circles* (Springer-Verlag, 2004).
- [41] G. Strona, D. Nappo, F. Boccacci, S. Fattorini, and J. San-Miguel-Ayanz, *Nature communications* **5**, 1 (2014).